

(1*Z*,3*Z*)-1,4-Di(pyridin-2-yl)buta-1,3-diene-2,3-diol: The Planar Highly Conjugated Symmetrical Ene-diol with Multiple Intramolecular Hydrogen Bonds

Borys Ośmiałowski,[†] Erkki Kolehmainen,[‡] Maija Nissinen,[‡] Tadeusz M. Krygowski,[§] and Ryszard Gawinecki^{*†}

Department of Chemistry, Technical and Agricultural University, Seminaryjna 3, PL-85-326 Bydgoszcz, Poland, Department of Chemistry, University of Jyväskylä, P.O. Box 35, FIN-40351 Jyväskylä, Finland, and Department of Chemistry, University of Warsaw, Pasteura 1, PL-02-093 Warsaw, Poland

gawiner@mail.atr.bydgoszcz.pl

Received November 19, 2001

¹H, ¹³C, and ¹⁵N NMR spectral data show that in chloroform solution (1*Z*,3*Z*)-1,4-di(pyridin-2-yl)buta-1,3-diene-2,3-diol, **OO**, is in ca. 9:1 equilibrium with (3*Z*)-3-hydroxy-1,4-di(pyridin-2-yl)but-3-en-2-one, **OK**, while no 1,4-di(pyridin-2-yl)-2,3-butanedione, **KK**, was detected. The species present in the tautomeric mixture were identified by comparing their experimental chemical shifts with those known for similar compounds as well as with the theoretically calculated (GIAO-HF/DFT) values. Ab initio calculations show that **OK** and especially the highly conjugated **OO** forms are preferred in the tautomeric mixtures both in vacuo and in chloroform solution. Comparison of experimental (Arrhenius) and calculated (ab initio) energies of **OK** shows that the MP2/6-31G^{**//}RHF/6-31G^{**} method gives the most precise results. There are one and two strong O–H···N hydrogen bonds present in the molecules of the former and latter compound, respectively. Other tautomeric forms, e.g., dienaminedione [(1*Z*,4*Z*)-1,4-di[pyridin-2(1*H*)-ylidene]butane-2,3-dione], and their rotamers were found to have higher energies. The single-crystal X-ray diffraction studies show that dienediol **OO** is the only tautomeric form present in the crystal at 173 K. Its almost perfectly planar molecule is stabilized by two strong intramolecular O–H···N hydrogen bonds.

Introduction

Covalent bonds are certainly much stronger than noncovalent interactions. It is known, however, that these weak forces, especially hydrogen bonding, affect considerably the structures of (molecular) crystals and liquids, as well as biomacromolecules such as DNA and proteins.¹ Tautomerism indicates that the studied compound is contaminated with or completely predominated by its isomer(s). The significance of that phenomenon in life-important processes is well-known.^{2–4}

An insignificant amount of the enol form is usually present in solutions of simple ketones.⁵ Although electron-withdrawing groups in the molecule increase the population of this tautomer, an aqueous solution of *p*-nitroacetophenone contains less than 0.01% of the enol at 298 K.⁶ It is also known that at the same temperature content of the enol form, RC₆H₄CH=C(OH)CH₃, in methanol solutions of phenylacetones, RC₆H₄CH₂COCH₃, is 0.8 and 8.4% for R = *p*-OMe and *p*-NO₂, respectively.⁷ These

numbers still seem high owing to the lack of stabilization of that tautomer by an intramolecular hydrogen bond. Such stabilization is possible, e.g., in (*Z*)-2-(2-hydroxy-2-phenylvinyl)pyridines.⁸

Butane-2,3-dione is in a tautomeric equilibrium with 1-buten-2-ol-3-one and 1,3-butadiene-2,3-diol, which are expected to be stabilized by the –OH···O=C< and –OH···O(H)– intramolecular hydrogen bonds. It is known, however, that enolization of acyclic 1,2-diketones is of minor importance.⁹ ¹H NMR spectra confirm that butane-2,3-dione is the major tautomeric form.¹⁰ 1,3-Butadiene-2,3-diols fit the definition of enediols.¹¹ Such compounds are more stable if there are bulky aromatic groups present in the molecule¹¹ or if there is a carbonyl group conjugated with the enolic C=COH moiety.¹² Since these two factors usually do not contribute in simple 1,3-butadiene-2,3-diols, the respective enediols are unstable compounds. Studies show that 1,4-diphenyl-2,3-butanedione, PhCH₂COCOCH₂Ph, is in equilibrium with 3-hydroxy-1,4-diphenylbut-3-en-2-one, PhCH=C(OH)COCH₂–

[†] Technical and Agricultural University.

[‡] University of Jyväskylä.

[§] University of Warsaw.

(1) Müller-Dethlefs, K.; Hobza, P. *Chem. Rev.* **2000**, *100*, 143.

(2) Elguero, J.; Marzin, C.; Katritzky, A. R.; Linda, P. *The Tautomerism of Heterocycles (Adv. Heterocycl. Chem., Supplement 1)*; Academic Press: New York, 1976.

(3) Katritzky, A. R.; Lagowski, J. M. *Adv. Heterocycl. Chem.* **1963**, *1*, 339.

(4) Katritzky, A. R.; Karelson, M.; Harris, P. A. *Heterocycles* **1991**, *32*, 329.

(5) Toulecc, J. Keto–enol equilibrium constants. In *The Chemistry of Enols*; Rappoport, Z., Ed.; Wiley: Chichester, 1990; pp 323–398.

(6) Toulecc, J. *Tetrahedron Lett.* **1984**, *25*, 4401.

(7) Zieliński, W.; Mazik, M. *Polish J. Chem.* **1992**, *66*, 661.

(8) Kolehmainen, E.; Ośmiałowski, B.; Nissinen, M.; Kauppinen, R.; Gawinecki, R. *J. Chem. Soc., Perkin Trans. 2* **2000**, 2185.

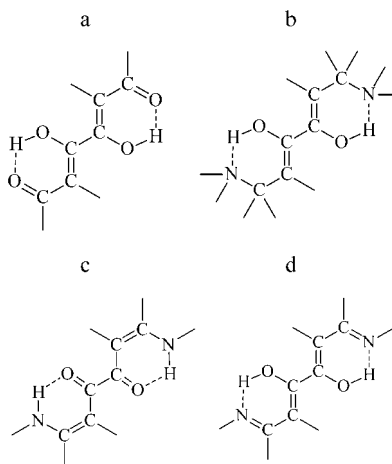
(9) Floris, B. NMR, IR conformation, and hydrogen bonding. In *The Chemistry of Enols*; Rappoport, Z., Ed.; Wiley: Chichester, 1990; pp 147–305.

(10) Blackburn, C.; Childs, R. F.; Kennedy, R. A. *Can. J. Chem.* **1983**, *61*, 1981.

(11) Hart, H.; Rappoport, Z.; Biali, S. E. Isolable and relatively stable simple enols. In *The Chemistry of Enols*; Rappoport, Z., Ed.; Wiley: Chichester, 1990; pp 481–589.

(12) Gilli, G.; Bertolasi, V. Structural Chemistry. In *The Chemistry of Enols*; Rappoport, Z., Ed.; Wiley: Chichester, 1990; pp 713–764.

Chart 1



Ph.¹³ The ¹H NMR supported evaluation shows that the tautomeric mixture in chloroform solution contains ca. 20% of mono-enol.¹³ On the other hand, titration of the ethanolic solution with bromine shows that diketone is probably contaminated with both mono- and dienol, PhCH=C(OH)C(OH)=CHPh.¹⁰ Further, this highly conjugated compound was obtained in a pure form by recrystallization from benzene.¹⁴

Formation of the strong hydrogen bond is also expected to be responsible for stabilization of 1,6-diketohexa-3,4-dienediols (a in Chart 1).^{15–17} On the other hand, it is noteworthy that resonance interactions are not necessary to stabilize enols. Some dihydroxydiallylamines (b in Chart 1) are also known.¹⁸ Although the respective dienaminodione tautomer (c in Chart 1) was found to be present in solution,¹⁹ additional proof is needed to distinguish it from diiminedienol (d in Chart 1).

Steric hindrance in the molecule of hexane-1,3,4,6-tetraone, RCOCH₂COCOCH₂COR (R = alkyl or aryl), is believed to be responsible for the lack of this form in solution.²⁰ Instead, there is a fast proton exchange between diketodienediols (a in Chart 1) and 2-hydroxy-2-acylmethyl-3(2H)-furanone (the minor tautomer).²⁰ 1,4-Di(pyridin-2-yl)-2,3-butanedione is an unusual α -diketone. It is expected to equilibrate with (3Z)-3-hydroxy-1,4-di(pyridin-2-yl)but-3-en-2-one and (1Z,3Z)-1,4-di(pyridin-2-yl)buta-1,3-diene-2,3-diol [*s-trans*-2,3-dihydroxy-1,4-di(pyridin-2-yl)-buta-1,3-diene]. Geometry and stability of these compounds and their tautomers as well as rotamers seem worthy of study.

Results and Discussion

NMR Spectra. The tautomers/rotamers of 1,4-di(pyridin-2-yl)-2,3-butanedione being considered in the

present paper are shown in Chart 2. The numbering of the positions in the molecule is exemplified in Chart 3.

The diketo forms, **KK**, are not present in chloroform solution. The chemical shifts of H7 at 303 K are 6.49 and 6.36 ppm (Table 1) for **OK** and **OO**, respectively. On the other hand, the H7' signal of **OK** is seen at 4.39 ppm. Integration of these two signals enables evaluation of the amount of dienol form in the solution ($91.2 \pm 0.5\%$). Due to slow proton transfer between **OO** and **OK**, both tautomeric forms are seen in the NMR spectra. The hydroxy groups in **OO** and **OK** are identified by the chemical shifts of the respective protons (δ 14.69).

Lower temperatures were found to decrease the amount of **OK** (**KK** was not detected). Thus, there is only 7.0% of this form at 223 K. Freezing of the solution results in separation of the signals of the protons in both tautomers. Thus, at 223 K the chemical shifts of the hydroxy protons are 15.37 and 15.33 ppm for **OO** and **OK**, respectively.

It is noteworthy that the ¹⁵N NMR chemical shift of **OO** (Table 1) is typical for the enolimine form.⁸ The ¹³C NMR chemical shifts are also helpful for identification of the forms present in solution. This was clearly proved for 2-phenacylpyridines and (*Z*)-2-(2-hydroxy-2-phenylvinyl)pyridines.⁸ The chemical shift of C7 in **OO** is ca. 100 ppm, whereas the respective value for the methylene carbon atom in **OK** is much less (47 ppm). There is also a sharp difference between the positions of C8 and C8' signals for this tautomer. Thus, these enolic and carbonyl carbon atoms are seen at ca. 158 and 196 ppm, respectively (Table 1).

Due to the low solubility of the tautomers in benzene-*d*₆, only some signals can be seen in the ¹H and ¹³C NMR spectra of the species present in solution. The chemical shifts show that **OO** is probably the major tautomer. In general, they are comparable to those in deuteriochloroform but except those for H7, H7', H9, and H9', all other ¹H NMR signals are more shielded in the latter solvent (Table 1). At 303 K, the content of dienol **OO** in C₆D₆ is comparable with that in chloroform ($92.3 \pm 0.5\%$).

Comparison of the δ (H9) values for **OO** (Table 1) and (*Z*)-2-(2-hydroxy-2-phenylvinyl)pyridines⁸ shows that there is a strong –OH \cdots N hydrogen bond present in both compounds. Such a case is often called RAHB, i.e., the resonance-assisted hydrogen bond.²¹ This seems to be a very important support for the stability of **OO**. It should be said, however, that this compound is also stabilized by the extent of conjugation in its molecule. Similar intramolecular interactions take place in *trans*-1,2-di(pyridin-2-yl)-1,2-ethenediol, predominating over α -pyridoin^{22,23} (Scheme 1). The signal of the hydroxy protons in the NMR spectrum of *trans*-1,2-di(pyridin-2-yl)-1,2-ethenediol was seen at 12.8 ppm (solution in CDCl₃).²³ Since the chemical shift of H9 is equal to 14.69 ppm for **OO**, the intramolecular hydrogen bonds in this compound seem to be much stronger than those in *trans*-1,2-di(pyridin-2-yl)-1,2-ethenediol.

Experimental ¹H, ¹³C, and ¹⁵N NMR chemical shifts are very helpful for distinguishing between different tautomeric forms.⁸ The GIAO-calculated chemical shifts can be even more helpful, especially if one is going to see

(13) Armani, V.; Dell'Erba, C.; Novi, M.; Petrillo, G.; Tavani, C. *Tetrahedron* **1997**, *53*, 1751.

(14) Ruggli, P.; Zeller, P. *Helv. Chim. Acta* **1945**, *28*, 741.

(15) Saalfrank, R. W.; Löw, N.; Demleitner, B.; Stalke, D.; Teichert, M. *Chem. Eur. J.* **1998**, *4*, 1305.

(16) Stachel, H.-D.; Schorp, M.; Maier, L.; Dandl, K. *Liebigs Ann. Chem.* **1994**, 1121.

(17) Shigorin, D. N.; Rudenko, N. A.; Chetkina, L. A.; Konshina, L. O.; Andreichikov, Yu. S.; Kozlov, A. P.; Murotsev, V. I.; Barashkov, N. N.; Lebedev, S. A. *Zh. Fiz. Khim.* **1992**, *66*, 2128.

(18) Hocker, J.; Merten, R. *Angew. Chem.* **1972**, *84*, 1022.

(19) Bonacorso, H. G.; Mack, K.-E.; Effenberger, F. *J. Heterocycl. Chem.* **1995**, *32*, 57.

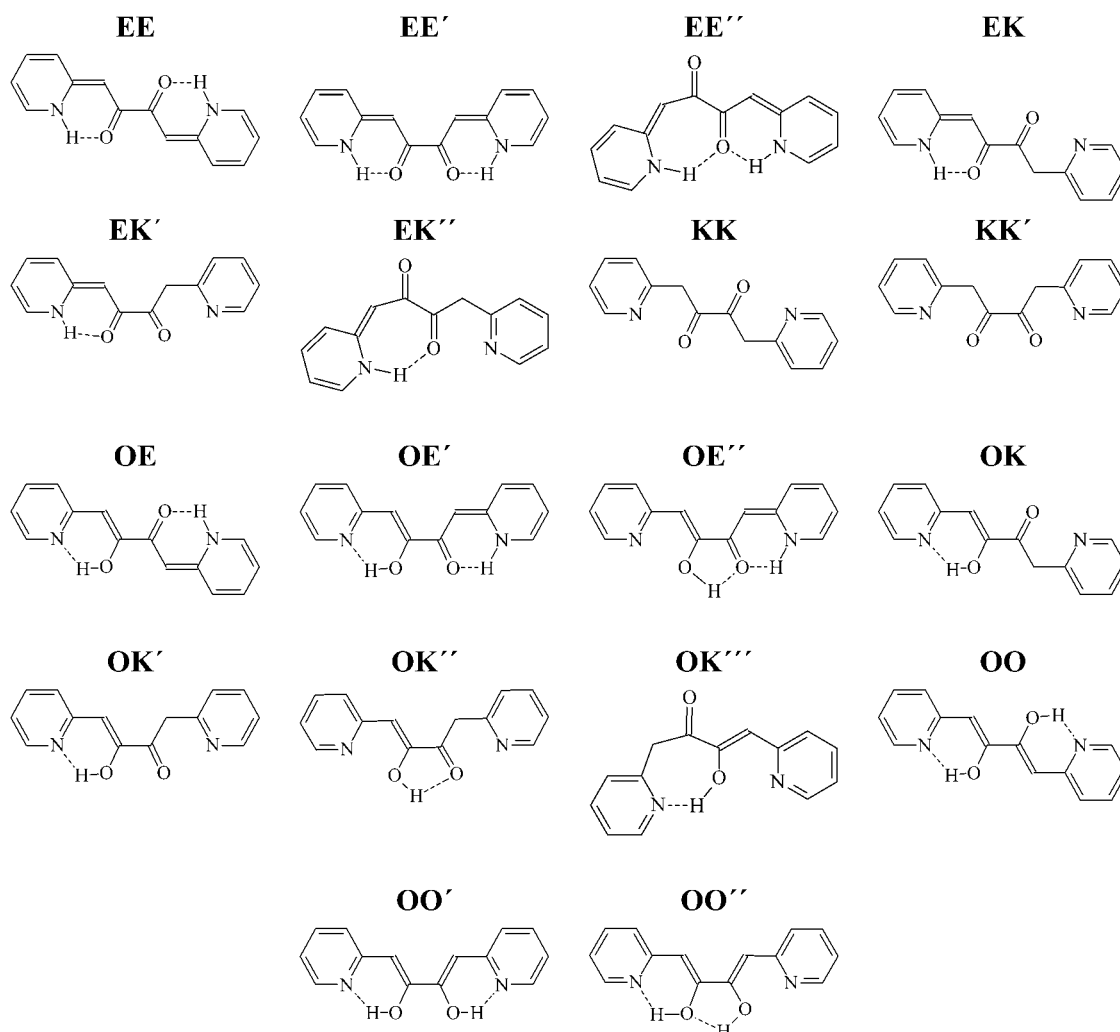
(20) Poje, M.; Balenovic, K. *J. Heterocycl. Chem.* **1979**, *16*, 417.

(21) Gilli, P.; Bertolasi, V.; Ferretti, V.; Gilli, G. *J. Am. Chem. Soc.* **2000**, *122*, 10405.

(22) Buehler, C. A. *Chem. Rev.* **1964**, *64*, 7.

(23) Brown, J. N.; Jenevein, R. M.; Stocker, J. H.; Trefonas, L. M. *J. Org. Chem.* **1972**, *37*, 3712.

Chart 2



which conformer predominates in the tautomeric mixture.²⁴ Thus, different high-level ab initio calculations, i.e., B3LYP/6-311G//RHF/3-21G, B3LYP/6-311G//RHF/6-31G**, and B3LYP/6-311G**//RHF/6-31G**, were performed to predict the respective values in the NMR spectra of the **OO** and **OK** forms. The B3LYP/6-311G//RHF/3-21G method gives the ¹H NMR chemical shifts that fit best with the experimental values with the highest accuracy. A similar result was obtained by us previously.²⁴ Three methods were used give the comparable ¹³C NMR chemical shifts. Moreover, the agreement between the calculated and experimental ¹H and ¹³C chemical shifts is better for **OO** than for **OO'**. Calculations show that both **OK** and **OK'** can be expected to appear in solution. However, much higher energy of **OK'** (as compared to that of **OK**, see Table 2 and Figure 1) excludes the presence of the latter tautomer.

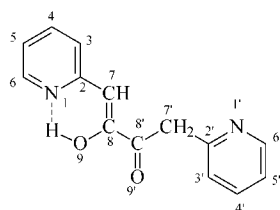
For two tautomers with the lowest energy obtained from MP2/6-31G**//RHF/6-31G** calculations, the more

advanced methods (MP2/6-31G**//MP2/6-31G**, MP2/6-31G**//B3LYP/6-31G**, and B3LYP/6-31G**//B3LYP/6-31G**, single-point calculations, PCM model of solvation) were also applied. The relative energy of **OK** in vacuo was found to be 4.96, 6.00, and 25.12 kJ/mol, respectively. Solvent (chloroform) decreases these values to 1.62, 2.23, and 20.10 kJ/mol, respectively. Since the content of **OK** in solution is 8.8% at 303 K, the Arrhenius relative energy of **OK** is 5.89 kJ/mol. It can be seen from Table 2 that the less sophisticated MP2/6-31G**//RHF/6-31G** (include PCM model of solvation) method approximates the experimental energy with the highest accuracy.

Experimental and calculated ¹⁵N NMR chemical shifts differ significantly from each other. It is known, however, that the strong interaction of the unshared electron pair of the nitrogen atom with the solvent is responsible for these differences.²⁵ On the other hand, experimental and calculated ¹H and especially ¹³C NMR chemical shifts correlate very well with each other (correlation coefficients are usually higher than 0.99). It is noteworthy that the calculated chemical shifts are only slightly dependent on conformation of the tautomeric form.

Calculations. The ab initio (RHF/6-31G**) method was used to optimize the geometries of different tau-

Chart 3



(24) Ośmiałowski, B.; Kolehmainen, E.; Gawinecki, R. *Magn. Reson. Chem.* **2001**, *39*, 334.

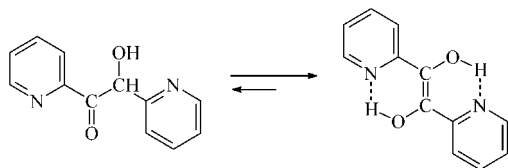
(25) Witanowski, M.; Biedrzycka, Z.; Grabowski, Z. *Magn. Reson. Chem.* **2000**, *38*, 580.

Table 1. Experimental ^1H , ^{13}C , and ^{15}N NMR Chemical Shifts (δ) of Different Tautomers for 0.1–0.2 M Solutions in CDCl_3 and C_6D_6 (Italic) at 303 K^a

	OO	OK		OO	OK
N1	-112.4	<i>b</i>	C8	158.36	156.85
N1'	-112.4	<i>b</i>		<i>158.97</i>	<i>b</i>
C2	158.44	157.69	C8'	158.36	196.14
	<i>159.40</i>	<i>b</i>		<i>158.97</i>	<i>b</i>
C2'	158.44	155.16	H3	7.13	7.24
	<i>159.40</i>	<i>b</i>		<i>6.55</i>	<i>6.99</i>
C3	122.55	124.01	H3'	7.13	7.25
	<i>122.94</i>	<i>b</i>		<i>6.55</i>	<i>6.98</i>
C3'	122.55	124.43	H4	7.64	7.62
	<i>122.94</i>	<i>b</i>		<i>6.83</i>	<i>c</i>
C4	137.18	136.53	H4'	7.64	7.65
	<i>137.21</i>	<i>b</i>		<i>6.83</i>	<i>c</i>
C4'	137.18	137.58	H5	7.03	7.12
	<i>137.21</i>	<i>b</i>		<i>6.28</i>	<i>c</i>
C5	119.45	120.96	H5'	7.03	7.12
	<i>119.74</i>	<i>b</i>		<i>6.28</i>	<i>b</i>
C5'	119.45	121.81	H6	8.35	8.39
	<i>119.74</i>	<i>b</i>		<i>7.79</i>	<i>7.64</i>
C6	145.14	145.32	H6'	8.35	8.57
	<i>146.10</i>	<i>b</i>		<i>7.79</i>	<i>8.43</i>
C6'	145.14	149.44	H7	6.36	6.49
	<i>146.10</i>	<i>b</i>		<i>6.80</i>	<i>c</i>
C7	96.96	100.68	H7'	6.36	4.39
	<i>98.50</i>	<i>b</i>		<i>6.80</i>	<i>4.45</i>
C7'	96.96	46.99	H9 (H9')	14.69 ^d	14.69 ^d
	<i>98.50</i>	<i>b</i>		<i>14.92^d</i>	<i>14.92^d</i>

^a See the Experimental Section for the reference compounds.

^b Not observed due to lower solubility in benzene. ^c These signals are probably overlapped with other signals. ^d Broad singlet.

Scheme 1

tomers (Chart 2). Diketo form **KK** is significantly twisted around the C2–C7 bond. The O9C8C8'O9' and C2C7C8O9 dihedral angles in **KK** are different from 180°. Twisting around the C2'–C7' and C7'–C8' bonds can also be seen in the keto moiety of the asymmetric forms such as **EK** and **OK**. On the other hand, the **E** fragments are planar. The initial C8C8'O9H angle in **OE''** was set to 0° in order to enable formation of the intramolecular >C=O...HO–hydrogen bond.

Strong repulsion between two carbonyl oxygen atoms in the *s-cis*-**EE'** rotamers results in a significant twist around the C8–C8' bond. Energetic preferences also cause twisting around the C8–C8' bond in the **OE'** and **OO'** forms. It is noteworthy that conformation of the pyridine rings with respect to the central part of the molecule was also subjected to the geometry optimization procedure.

RHF/6-31G** calculations show that the diketo form **KK** is preferred in vacuo, whereas more sophisticated methods including both electron correlation (MP2/6-31G**) and solvent effect (PCM model of solvation) show that **OK** and especially highly conjugated **OO** forms predominate in the tautomeric mixtures in chloroform solution (Figure 1 and Table 2). The dienaminone form **EE''** was found to have the highest energy. The energy differences between **OO** and **EE''** for the pyridine derivative are equal to 96.46 and 89.68 kJ/mol in vacuo and in solution, respectively. The data in Table 2 show that the

difference between **OO** and **OK** is more distinct in vacuo than in solution. The difference between **OO** and **OK** is equal to 3.63 and 7.05 kJ/mol for these two species (in chloroform), respectively. The energy of the **OO'** rotamer is much higher than that of **OK**. Thus, it is clearly seen that the most stable tautomers are populated mainly with **EE**, **EK**, and **OE** in which the pyridine moieties are linked to the side chain by the double bond(s).

It seems worthy to discuss the effect of symmetry on the energy of highly conjugated symmetrical molecules. Thus, **OO** and **EE** have the perpendicular plane of symmetry. The energies of the **EE** forms are higher than these of **OO**. Thus, the symmetry of the molecule is not as important as the type of tautomer (dienol predominates over dienaminone). Other highly conjugated tautomers, e.g., **OE** and **OE'**, must be considered, too. There is neither center nor plane of symmetry in their molecules. The energy of these tautomers is intermediate between those for **OO** and **EE**: $E_{OO} < E_{OE} < E_{EE}$ and $E_{OO'} < E_{OE'} < E_{EE'}$. On the other hand, $E_{OO} < E_{OO'}$, $E_{EE} < E_{EE'}$ and $E_{OE} < E_{OE'}$. Thus, the “less symmetric” **OO'**, **OE'**, and **EE'** tautomers/rotamers are expected to be absent in the tautomeric mixtures.

Figure 2 shows that the energetic dependence of **OO** on the O–H bond length (calculations at the MP2/6-31G**//RHF/6-31G** level and PCM model of solvation). The molecule has the minimum energy for $d_{OH} = 100.3$ pm. It is noteworthy that extension of the O–H to 120 pm causes only a relatively insignificant increase in energy: $\Delta E = 39.16$ kJ/mol.

It can be seen in Table 3 that the less stable enaminone forms have the highest solvation energies. Since high solvation energy may cause the intramolecular hydrogen bonds to be broken in the solution, these in the enol forms, especially in **OO**, seem to be very strong.

X-ray Data. The X-ray diffraction studies show that enediol **OO** is the only tautomeric form present in the crystal at 173.0 K (Figure 3). The molecule is almost perfectly planar. This tautomeric form is stabilized by two strong hydrogen bonds, $d(O9\cdots N1) = 261.9(6)$ pm and $d(O9'\cdots N1') = 258.0(6)$ pm. The molecule has no perpendicular symmetry plane. Comparison of the X-ray data with the calculated values (Table 4) shows that molecular geometry is best estimated by the MP2/6-31G** method. However, the correlation coefficients for the linear dependences between experimental and theoretical parameters are the same for three methods used (0.99 for bond lengths and 0.90 for valence angles), the sum of the absolute differences between experimental and theoretical values, $\Sigma|\Delta|$, is equal to 82.6, 44.3, and 42.6 pm (bond lengths and inter atomic distances), and 21.8, 18.3, and 17.8° (valence angles), for RHF/6-31G**, B3LYP/6-31G**, MP2/6-31G** methods, respectively.

Since the intramolecular bonds are strong, no intermolecular hydrogen bonding is possible. Thus, the packing of the molecules of enediol **OO** in crystalline state is affected mainly by π -stacking. The molecules pack into slightly offset face-to-face dimeric pairs with the closest intermolecular π -stacking distances being C2–C3'–1 = 349.0(6), C3–C4'–1 = 351.5(6), C7–C2'–1 = 352.5(6) and C8–C7'–1 = 352.6(6) pm. The dimeric pairs adopt further an almost perpendicular arrangement in respect to each other (Figure 4) stabilized by the weaker edge-to-face π -interactions (the closest carbon-to-carbon distances vary from 360 to 400 pm).

Table 2. Calculated Relative Energies at the MP2/6-31G**//RHF/6-31G** Level (kJ/mol) for Different Tautomers/Rotamers

tautomer	in vacuo	in chloroform ^a	tautomer	in vacuo	in chloroform
EE	61.77	56.33	OE'	50.98	44.43
EE'	87.57	77.95	OE''	71.47	63.65
EE''	96.46	89.68	OK	4.92	3.63
EK	34.94	30.54	OK'	24.03	18.73
EK'	61.00	51.67	OK''	47.89	42.80
EK''	76.37	73.22	OK'''	84.81	76.19
KK	21.29	19.27	OO	0.00	0.00
KK'	45.80	40.62	OO'	19.68	16.96
OE	29.90	26.92	OO''	60.61	55.68
<i>b</i>	-798.296 278 1	-798.298 582			

^a PCM model of solvation. ^b Energy (au) of the most stable tautomer.

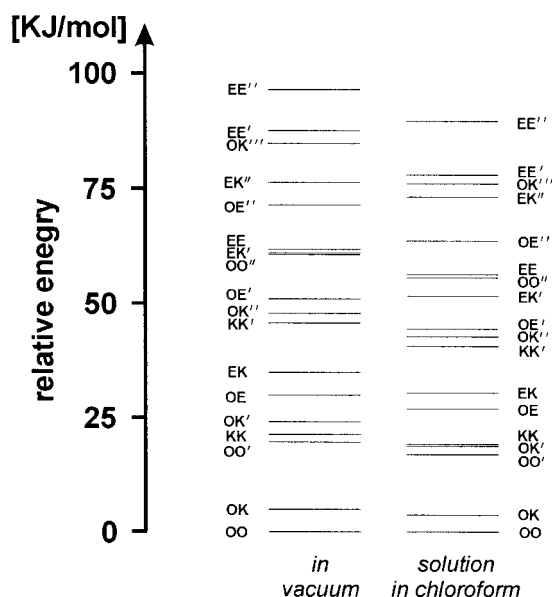


Figure 1. Relative energies of different tautomers/rotamers in vacuo and in chloroform solution calculated with MP2/6-31G** method at the geometry obtained with the RHF/6-31G** method and the same basis sets (PCM model of solvation).

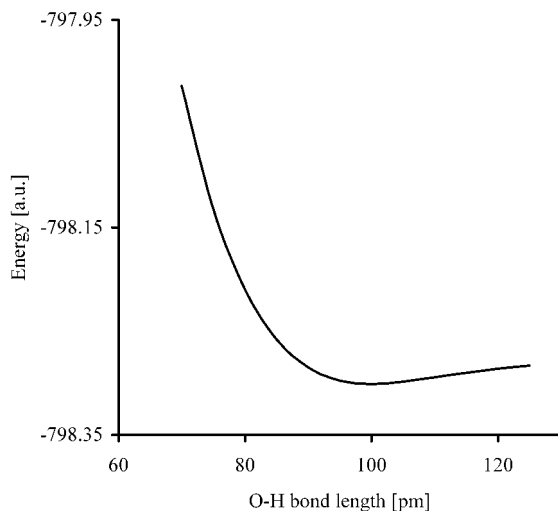


Figure 2. Energetic dependence of **OO** on the O-H bond length.

Conclusions

(1*Z*,3*Z*)-1,4-Di(pyridin-2-yl)buta-1,3-diene-2,3-diol, **OO**, is in equilibrium with (3*Z*)-3-hydroxy-1,4-di(pyridin-2-yl)but-3-en-2-one, **OK**. Other possible tautomers, i.e., 1,4-di(pyridin-2-yl)butane-2,3-dione, **KK**, (1*Z*,4*Z*)-1,4-di[py-

Table 3. Calculated Solvation Energies^a (kJ/mol) for Different Tautomers/Rotamers

tautomer	energy	tautomer	energy
EE	-11.49	OE'	-12.61
EE'	-15.67	OE''	-13.87
EE''	-12.83	OK	-7.34
EK	-10.44	OK'	-11.35
EK'	-15.39	OK''	-11.14
EK''	-9.21	OK'''	-14.67
KK	-8.07	OO	-6.05
KK'	-11.22	OO'	-8.77
OE	-9.03	OO''	-10.98

^a Differences between the MP2/6-31G**//RHF/6-31G** (PCM solvation model) and MP2/6-31G**//RHF/6-31G** (in vacuo) calculated energies.

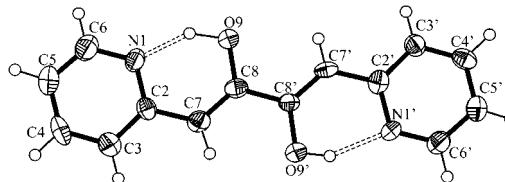


Figure 3. ORTEP-3²⁶ plot of the crystal structure of (1*Z*,3*Z*)-1,4-di(pyridin-2-yl)buta-1,3-diene-2,3-diol (**OO**). The thermal ellipsoids are drawn by 50% probability level.

ridin-2(*1H*)-ylidene]butane-2,3-dione, **EE**, (4*Z*)-1-pyridin-2-yl-4-pyridin-2(*1H*)-ylidenbutane-2,3-dione, **EK**, and (1*Z*,3*Z*)-3-hydroxy-4-pyridin-2-yl-1-pyridin-2(*1H*)-ylidenbut-3-en-2-one, **OE**, are not present in chloroform solution. This finding is in contrast with the observation that an insignificant amount of the enol form is usually present in solutions of simple monoketones, e.g., benzophenone, and α -diketones, e.g., 1,4-diphenyl-2,3-butanedione. Conjugation and strong O-H...N hydrogen bonds present in the **OO** and **OK** molecules are responsible for the stability of these tautomers. Ab initio calculations including both electron correlation and solvent effect show that **OK** and especially the highly conjugated **OO** forms are preferred both in vacuo and in chloroform solution. Enediol **OO** is the only tautomeric form present in the crystal at 173.0 K. Its almost perfectly planar molecule is stabilized by two strong O-H...N hydrogen bonds. Our studies show that 1,2-diketone can be almost completely transformed into the respective enediol if it is stabilized by the conjugation and multiple intramolecular hydrogen bonds.

Experimental Section

Synthesis. (1*Z*,3*Z*)-1,4-Di(pyridin-2-yl)buta-1,3-diene-2,3-diol, mp 170–172 °C, was obtained by treating 2-lithiomethylpyridine (2 molar excess) with ethyl oxalate. Synthetic

Table 4. Selected Bond Lengths (pm) and Bond and Dihedral Angles (deg) for OO

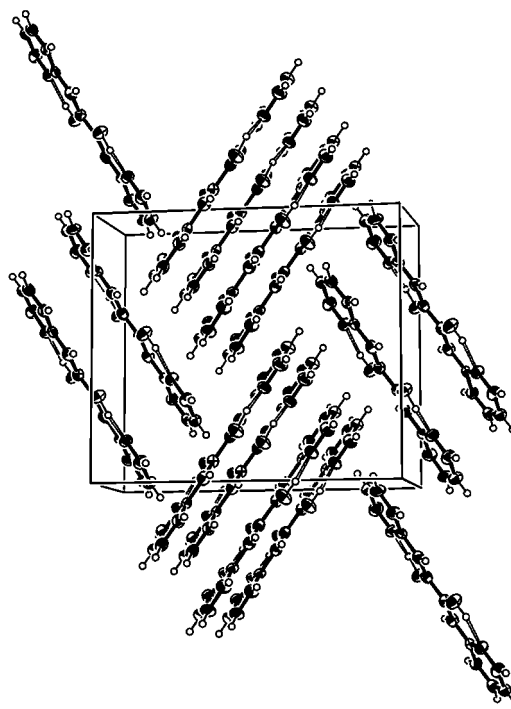
	X-ray	RHF/ 6-31G**	B3LYP/ 6-31G**	MP2/ 6-31G**
N1–C2	134.5(6)	133.2	136.1	136.2
N1'–C2'	135.6(6)	133.2	136.1	136.2
N1–C6	134.3(7)	132.2	133.7	134.3
N1'–C6'	132.2(7)	132.2	133.7	134.3
C2–C7	144.9(7)	146.4	144.6	144.6
C2'–C7'	144.4(7)	146.4	144.6	144.6
C7–C8	135.3(7)	133.8	136.7	136.6
C7'–C8'	133.3(7)	133.8	136.7	136.6
C8–O9	134.7(6)	133.1	134.1	135.0
C8'–C9'	135.8(6)	133.1	134.1	135.0
C8–C8'	146.9(7)	148.3	147.5	146.8
O9–H9	106(6)	95.6	100.4	99.7
O9'–H9'	91(6)	95.6	100.4	99.7
H9...N1	165(6)	187.1	168.8	171.4
H9'...N1'	178(6)	187.1	168.8	171.4
O9...N1	258.0(6)	269.7	259.9	261.7
O9'...N1'	261.9(6)	269.7	259.9	261.7
C2N1C6	117.8(5)	119.4	119.4	119.1
C2'N1'C6'	118.3(5)	119.4	119.4	119.1
N1C2C7	117.2(5)	118.9	117.9	117.9
N1'C2'C7'	117.5(6)	118.9	117.9	117.9
C2C7C8	124.5(5)	125.1	123.5	123.7
C2'C7'C8'	125.5(6)	125.1	123.5	123.7
C7C8O9	122.6(5)	125.0	123.7	124.2
C7'C8'O9'	123.2(5)	125.0	123.7	124.2
C7C8C8'	123.2(5)	121.4	121.5	121.5
O9H9N1	144(4)	143.0	148.7	148.6
O9'H9'N1'	151(5)	143.0	148.7	148.6
N1C2C7C8	1.6(8)	0.0	0.0	0.0
N1'C2'C7'C8'	–2.5(8)	0.0	0.0	0.0
C2C7C8O9	0.4(8)	0.0	0.0	0.0
C2'C7'C8'O9'	1.5(8)	0.0	0.0	0.0
O9C8C8'O9'	176.3(5)	180.0	180.0	180.0
C7C8C8'C7'	178.8(6)	180.0	180.0	180.0
C2C7C8C8'	178.6(5)	180.0	180.0	180.0
C2'C7'C8'C8'	–179.4(5)	180.0	180.0	180.0

procedure was that used recently.⁸ The crude product precipitated from the reaction mixture was further purified by the column chromatography [silica gel (230–400 mesh), hexane/ethyl acetate (9:1)] and recrystallization from aqueous ethanol. Satisfactory analytical data ($\pm 0.3\%$ for C, H, and N) were obtained.

NMR Spectra. All NMR spectra were recorded for 0.1–0.2 M CDCl₃ solutions at 303 K (unless otherwise stated) with a two-channel digital FT NMR spectrometer equipped with an inverse detection 5 mm diameter broad band probehead and z -gradient working at 500.13 MHz (¹H), 125.76 MHz (¹³C), and 50.59 MHz (¹⁵N). In ¹H NMR experiments, the spectral width was 8500 Hz (17 ppm), the number of data points 65 K, the flip angle 30°, and the number of scans 32. The FIDs were multiplied by an exponential window function of the digital resolution (0.13 Hz) prior to Fourier transform (FT). The ¹H NMR chemical shifts are referenced to the trace signal of CHCl₃ ($\delta = 7.26$ ppm from internal TMS).

In proton composite pulse decoupled (Waltz-16) ¹³C NMR experiments the spectral width was 30 300 Hz (240 ppm), the number of data points 65 K, the flip angle 30°, and the number of scans typically > 10 000 in order to observe reliably also the weak signals of the minor contributors. The FIDs were multiplied by an exponential window function of the digital resolution (0.92 Hz) prior to FT. The ¹³C NMR chemical shifts are referenced to the signal of CDCl₃ ($\delta = 77.00$ ppm from TMS).

To distinguish the spin systems belonging to the different rings and tautomeric forms as well as to assign the ¹H NMR spectra reliably the 2D double quantum filtered (DQF) ¹H, ¹H COSY^{27,28} experiments were also run. In these experiments, the spectral ranges were limited in aromatic parts (typically less than 1000 Hz), the data matrix size was 256 points (f_2 -axis) \times 128 points (f_1 -axis), which was zero filled to 256 points along the f_1 -axis prior to FT. Thirty-two scans were ac-

**Figure 4.** Molecular packing in the crystal structure of (1*Z*,3*Z*)-1,4-di(pyridin-2-yl)buta-1,3-diene-2,3-diol.

cumulated for every f_1 -increment (f_2 -spectrum). A shifted sine-bell window function was used along both axes prior to FT.

2D z -pulsed field gradient (PFG) selected ¹H, ¹³C HMQC^{29,30} and ¹H, ¹³C HMBC³¹ experiments were run to assign reliably the ¹³C NMR spectra. In HMQC, the matrix size was typically 2500 Hz/512 points (¹H = f_2 -axis) \times 10 000 Hz/512 points (¹³C = f_1 -axis), which was multiplied by a sine-bell window function along both axes prior to FT. The number of scans was 32, and a composite pulse decoupling (garp) was used to remove proton couplings. In HMBC measurements, 64 scans were accumulated for each f_1 -increment, and the matrix size and windowing were the same as in HMQC. A low-pass filter (to remove correlations transmitted via direct couplings) and a 50 ms delay [for an evolution of $^nJ(C,H)$ couplings] were included in the HMBC pulse sequence.

To determine the ¹⁵N NMR chemical shifts, z -PFG ¹H, ¹⁵N HMBC experiments were run. In these experiments, the size of the data matrix was 2500 Hz/512 points (¹H) \times 22 500 Hz/1024 points (¹⁵N-axis). The ¹⁵N NMR chemical shifts were referenced to an external nitromethane ($\delta = 0.0$ ppm) sample in a 1 mm diameter capillary tube inserted coaxially inside the 5 mm NMR sample tube. A sine-bell multiplication was done along both axes prior to FT. Sixty-four scans were accumulated for every ¹⁵N = f_1 -increment. A 100 ms delay for an evolution of $^nJ(N,H)$ couplings was included in this HMBC pulse sequence.

X-ray. The X-ray crystallographic data were recorded using graphite monochromatized Mo K α radiation [$\lambda(\text{Mo K}\alpha) = 71.073$ pm] and temperature of 173.0 \pm 0.1 K. The CCD data were processed with Denzo-SMN v0.93.0,³² and the structure was solved by direct methods (SIR-92³³) and refined on F^2 by full-matrix least squares techniques (SHELXL-97³⁴). Absorp-

(27) Rance, M.; Sørensen, O. W.; Bodenhausen, G.; Wagner, G.; Ernst, R. R.; Wüthrich, K. *Biochem. Biophys. Res. Commun.* **1984**, *117*, 479.

(28) Derome, A.; Williamson, M. *J. Magn. Reson.* **1990**, *88*, 177.

(29) Bax, A.; Griffey, R. H.; Hawkins, B. L. *J. Magn. Reson.* **1983**, *55*, 301.

(30) Bax, A.; Subramanian, S. *J. Magn. Reson.* **1986**, *67*, 565.

(31) Bax, A.; Summers, M. F. *J. Am. Chem. Soc.* **1986**, *108*, 2093.

(32) Otwinowski, Z.; Minor, W. *Methods Enzymol.* **1997**, *276*, 307.

(33) Altomare, A.; Casciaro, G.; Giacovazzo, C.; Guagliardi, A. *J. Appl. Crystallogr.* **1993**, *26*, 343.

tion correction was not used. The hydrogen atoms were located from the difference Fourier map but in the final refinement calculated to their idealized positions with isotropic temperature factors (1.2 times C temperature factor) except for hydrogens H9, H9', H7, and H7', which were located from the difference Fourier map but refined with fixed temperature factors. Due to the weak scattering power of very small organic crystal ($0.05 \times 0.05 \times 0.15$ mm) the *R* values of the structure are rather poor, however the conclusions about the crystal structure are still entirely justified.

Calculations. Ab initio calculations were carried out with the GAUSSIAN 98³⁵ program using the 6-31G** basis set at the RHF, B3LYP, and MP2 levels (geometry optimization). The

(34) Sheldrick, G. M. *SHELXL 97, A Program for Crystal Structure Refinement*; University of Göttingen: 1997.

(35) Frisch, M. J.; Trucks, G. W.; Schlegel, H. B.; Scuseria, G. E.; Robb, M. A.; Cheeseman, J. R.; Zakrzewski, V. G.; Montgomery, J. A.; Stratmann, R. E.; Burant, J. C.; Dapprich, S.; Millam, J. M.; Daniels, A. D.; Kudin, K. N.; Strain, M. C.; Farkas, O.; Tomasi, J.; Barone, V.; Cossi, M.; Cammi, R.; Mennucci, B.; Pomelli, C.; Adamo, C.; Clifford, S.; Ochterski, J.; Petersson, G. A.; Ayala, P. Y.; Cui, Q.; Morokuma, K.; Malick, D. K.; Rabuck, A. D.; Raghavachari, K.; Foresman, J. B.; Cioslowski, J.; Ortiz, J. V.; Baboul, A. G.; Stefanov, B. B.; Liu, G.; Liashenko, A.; Piskorz, P.; Komaromi, I.; Gomperts, R.; Martin, R. L.; Fox, D. J.; Keith, T.; Al-Laham, M. A.; Peng, C. Y.; Nanayakkara, A.; Challacombe, M.; Gill, P. M. W.; Johnson, B.; Chen, W.; Wong, M. W.; Andres, J. L.; Gonzalez, C.; Head-Gordon, M.; Replogle, E. S.; Pople, J. A. Gaussian 98, Revision A.9; Gaussian, Inc.: Pittsburgh, PA, 1998.

PCM model was applied in simulation of the solvent effect.^{36,37} The GIAO calculations for the ¹³C chemical shifts were performed at the B3LYP/6-311G and 6-311G** levels for geometry obtained from the RHF/3-21G and RHF/6-31G** optimizations.

Acknowledgment. We are very much indebted to the CYFRONET Regional Computing Center of S. Staszic University of Mining and Metallurgy in Cracow for the supply of computer time and for providing programs (Grant No. KBN/SGI-ORIGIN-2000/ATRBydg/072/2000). This work was supported by the Polish National Research Council (KBN), Grant No. 7 T09A 128 20. One of us (B.O.) gratefully acknowledges receipt of a Fellowship from the Foundation for Polish Science (FNP). Special Laboratory Technician Reijo Kauppinen is acknowledged for his help with the NMR experiments.

Supporting Information Available: Optimized geometries, GIAO-calculated chemical shifts of the tautomers, and X-ray crystallographic data. This material is available free of charge via the Internet at <http://pubs.acs.org>.

JO016293B

(36) Miertus, S.; Tomasi, J. *Chem. Phys.* **1982**, *65*, 239.

(37) Miertus, S.; Scrocco, E.; Tomasi, J. *Chem. Phys.* **1981**, *55*, 117.